



**HAL**  
open science

## Highly heterogeneous morphology of cobalt oxide nanostructures for the development of sensitive and selective ascorbic acid non-enzymatic sensor

Abdul Sattar Chang, Aneela Tahira, Fouzia Chang, Abdul Ghaffar Solangi, Muhammad Ali Bhatti, Brigitte Vigolo, Ayman Nafady, Zafar Hussain Ibupoto

### ► To cite this version:

Abdul Sattar Chang, Aneela Tahira, Fouzia Chang, Abdul Ghaffar Solangi, Muhammad Ali Bhatti, et al. Highly heterogeneous morphology of cobalt oxide nanostructures for the development of sensitive and selective ascorbic acid non-enzymatic sensor. *Biosensors*, 2023, 13 (1), pp.147. 10.3390/bios13010147 . hal-04197512

**HAL Id: hal-04197512**

**<https://hal.univ-lorraine.fr/hal-04197512>**

Submitted on 6 Sep 2023

**HAL** is a multi-disciplinary open access archive for the deposit and dissemination of scientific research documents, whether they are published or not. The documents may come from teaching and research institutions in France or abroad, or from public or private research centers.

L'archive ouverte pluridisciplinaire **HAL**, est destinée au dépôt et à la diffusion de documents scientifiques de niveau recherche, publiés ou non, émanant des établissements d'enseignement et de recherche français ou étrangers, des laboratoires publics ou privés.

# Highly heterogeneous morphology of cobalt oxide nanostructures for the development of sensitive and selective ascorbic acid non-enzymatic sensor

Abdul Sattar Chang<sup>1</sup>, Aneela Tahira<sup>3</sup>, Fouzia Chang<sup>4</sup>, Abdul Ghaffar Solangi<sup>3</sup>, Muhammad Ali Bhatti<sup>5</sup>, Brigitte Vigolo<sup>6</sup>, Ayman Nafady\*<sup>2</sup>, Zafar Hussain Ibupoto\*<sup>1</sup>

<sup>1</sup>Dr. M.A Kazi Institute of Chemistry University of Sindh Jamshoro, 76080, Sindh Pakistan

<sup>2</sup> Department of Chemistry, College of Science, King Saud University, Riyadh 11451, Saudi Arabia

<sup>3</sup>Institute of Chemistry, Shah Abdul Latif University of Khairpur Mirs, Sindh Pakistan

<sup>4</sup>National Centre of Excellence in Analytical Chemistry, University of Sindh Jamshoro, 76080, Sindh Pakistan

<sup>5</sup>Institute of Environmental Sciences, University of Sindh Jamshoro, 76080, Sindh Pakistan

<sup>6</sup>Université de Lorraine, CNRS, IJL, F-54000 Nancy, France

\***Corresponding authors.** Prof. Zafar Hussain Ibupoto, Email: zaffar.ibhupoto@usindh.edu.pk, Prof. Ayman Nafady, Email: anafady@ksu.edu.sa

## Abstract

The surface tailored metal oxide nanostructures for the development of non-enzymatic sensors are highly demanded but it's a big task due to wide range of complexities during the growth process. The presented study was focused on the surface modification of heterogeneous morphology of cobalt oxide (Co<sub>3</sub>O<sub>4</sub>) prepared by hydrothermal method. Further surface modification was done with the use of sodium citrate as a reducing and surface modifying agent for the Co<sub>3</sub>O<sub>4</sub> nanostructures through high density of oxygenated terminal groups from citrate ions. The citrate ions enabled a significant surface modification of Co<sub>3</sub>O<sub>4</sub> nanostructures which further improved the electrochemical properties of Co<sub>3</sub>O<sub>4</sub> material towards the design of non-enzymatic ascorbic acid sensor in phosphate buffer solution of pH 7.4. The morphology and crystal arrays of Co<sub>3</sub>O<sub>4</sub> nanostructures were studied by scanning electron microscopy (SEM) and

powder X-ray diffraction (XRD) techniques. These physical characterizations have shown highly tailored surface features of  $\text{Co}_3\text{O}_4$  nanostructures and significant impact on the crystal properties. The electrochemical activity of  $\text{Co}_3\text{O}_4$  was studied by chronoamperometry, linear sweep voltammetry, and cyclic voltammetry (CV) for the detection of ascorbic acid. The linear range of proposed sensor was measured from 0.5 mM to 6.5 mM and a low limit of detection of 0.001 mM was also estimated. The presented  $\text{Co}_3\text{O}_4$  nanostructures exhibited significant surface roughness and surface area, consequently played a vital role towards selective, sensitive and stable detection of ascorbic acid. The use of low cost surface modifying agent like sodium citrate could be of great interest for surface roughness and high surface area of nanostructured materials for the improved electrochemical properties for the biomedical, energy storage and conversion systems.

**Keywords:**  $\text{Co}_3\text{O}_4$  nanostructures, sodium citrate, non-enzymatic approach, ascorbic acid sensor,

## 1. Introduction

The physiological activities in the living organisms are intensively governed by the presence of ascorbic acid (Vitamin C) and the abnormal level of ascorbic acid concentration can severely affect the health and cause the scurvy followed by the collagen formation. The ascorbic acid is highly useful in our body for the skin, immune and tissue system developments [1]. Importantly, the ascorbic acid is strong antioxidant and it drives the metabolism of cholesterol effectively in human body [2], hence its accurate and sensitive determination is vital for the practical applications. The conventional methods have been used to determine the ascorbic acid from food and clinical samples [3, 4], and these methods include chromatographic[6,7], spectrophotometry[5], fluorimetry[6], NIR, MIR and FT-Raman techniques[7]. These conventional methods are associated with high cost, time taking, complicated, and require well skillful person for the ascorbic acid detection. Furthermore, electroanalytical methods such as voltammetry[8-11], amperometry[12] and potentiometric[13] have been used extensively due to their high potential, promising and advantageous features such as low cost, simple, highly sensitive and accurate towards the detection of analytes [14]. The electrochemical methods

have been used through two methodologies for the development of biosensors. First, the use of enzyme immobilization on electrocatalytic materials [15], dye immobilization[16], polymer coating [17] for the determination of ascorbic acid. The enzyme immobilization on the electrocatalytic materials is suffered by the poor thermal stability, enzyme spoilage, complicated enzyme immobilization process, and high consumption of substrate molecules [18]. Second, recently non-enzymatic methods are intensively used for the design of electrochemical sensors due to their several advantages such as highly sensitive, thermally stable, easy to operate, and fast response [19]. However, non-enzymatic methods require efficient electrocatalytic materials for the sensitive and selective detection of small biomolecules, hence this method is still at early stage its utilization for the practical applications. Thus, new studies are always welcome by the researchers and industrialists for the synthesis of new functional materials with enhanced electrocatalytic properties for the sensitive and selective electroanalytical applications. Among the materials, transition metal oxides are a unique class of materials, due to unique d-orbital configuration for the tailored catalytic properties for the development of non-enzymatic sensors. The cobalt oxide ( $\text{Co}_3\text{O}_4$ ) among the transition oxides is highly investigated for the electrochemical applications since two decades due to its spinel structure and mixed oxidation states for swift redox reaction kinetics. Moreover, it is low cost, ecofriendly, and easy to prepare [20]. This is the reason,  $\text{Co}_3\text{O}_4$  nanostructures have been studied for the wide range of applications such as energy storage systems[21], heterogeneous catalysis[22], magneto resistive devices[23] and electrochromic thin films[24]. Beside these applications of  $\text{Co}_3\text{O}_4$  nanostructures, they have been potentially utilized for the development of electrochemical sensors [25]. For example,  $\text{Co}_3\text{O}_4$  nanostructures have been employed for the development of glucose[26, 27], lactic acid[28], ascorbic acid[29] and urea[30] electrochemical sensors. The improvement in the electrocatalytic properties of  $\text{Co}_3\text{O}_4$  nanostructures have been done by various methods such as doping, developing composite structures, and surface modifications using different preparation methods [19, 20, 31, 32]. Despite these extensive efforts, the electrochemical performance of  $\text{Co}_3\text{O}_4$  nanostructures is found poor towards the fabrication of efficient non-enzymatic electrochemical sensors and their realization in real sample analysis. Therefore, new type of simple and low cost approaches for the synthesis of  $\text{Co}_3\text{O}_4$  nanostructures have to be studied for the development of new generation of non-enzymatic ascorbic acid sensors. The use of oxygen rich oxygen terminated atoms of anionic species such as citrate, can be effectively evolve the morphology and change the number of surface active sites on the

surface of material for enhanced electrochemical properties of  $\text{Co}_3\text{O}_4$  nanostructures. The use of rich oxygenated terminal groups for enabling the surface roughness of  $\text{Co}_3\text{O}_4$  nanostructures has not been studied elsewhere. For this reason, we have employed the sodium citrate due to its low cost reducing agent properties via oxygenated terminals for the  $\text{Co}_3\text{O}_4$  nanostructures. Furthermore in this study, we have highlighted the role of citrate ions from sodium citrate with abundant oxygen terminals for making the roughness on the surface of  $\text{Co}_3\text{O}_4$  nanostructures. Also, presented study has been carried out in different way compare to our previous studies, where we have utilized directly surface modifying agents in the precursors of nanostructured material [31, 32]. In those studies, we did not highlight the surface roughness factor by the use of low cost and mild reducing agent for the prepared nanostructured materials towards the development of non-enzymatic sensors. Hence, the proposed research work is completely different from our previous studies and such kind of strategy has not been reported to date. At the end, modified surface of  $\text{Co}_3\text{O}_4$  nanostructures played an important role for the sensitive and selective detection of ascorbic acid using non-enzymatic approach

## **2. Materials and methods**

### **2.1. Used chemicals**

Different chemicals such as cobalt sulfate, sodium citrate, urea, ascorbic acid, and 5% Nafion were purchased from Sigma Aldrich Karachi, Pakistan and all of them of were of high analytical grade. The preparation of desired solutions was done with the deionized water. Prior to experiments, the glassware was cleaned with deionized water and dried at room temperature. The phosphate buffer solution of pH 7.4 was made with the use of various salts such as 0.1mM  $\text{H}_3\text{PO}_4$ , 0.1mM  $\text{NaH}_2\text{PO}_4$ , 0.1mM  $\text{Na}_2\text{HPO}_4$  and 0.01mM  $\text{NaCl}$  in the deionized water. The pH of phosphate buffer solution was adjusted using 0.2 M  $\text{HCl}$  and  $\text{NaOH}$  aqueous solutions.

### **2.2. Hydrothermal preparation of $\text{Co}_3\text{O}_4$ nanostructures using sodium citrate as surface modifying agent**

First,  $\text{Co}_3\text{O}_4$  nanostructures were prepared by hydrothermal method followed by thermal annealing in air. The synthesis of  $\text{Co}_3\text{O}_4$  nanostructures was done with the use of cobalt precursor of 0.1 M cobalt sulfate and 0.1 M urea in 500 mL of deionized water. The well dispersion of cobalt precursor was obtained through mechanical stirring with glass rod for 10 min. Then, the

cobalt precursor solution was covered with aluminum sheet and hydrothermal process performed at 90 °C to 95 °C for 5 h. The prepared cobalt hydroxide material was collected on the ordinary filter paper and washed several times with the deionized water followed by drying at 60 °C for overnight. Then, the cobalt hydroxide phase material was kept in china clay made crucible and annealed at 500 °C for 4 h. Afterwards, a typical  $\text{Co}_3\text{O}_4$  nanostructures with black color were obtained and they were named as pristine  $\text{Co}_3\text{O}_4$  (sample 1). Secondly, the  $\text{Co}_3\text{O}_4$  nanostructures were treated with sodium citrate for the purpose of surface modification. The choice of sodium citrate was taken on the basis of rich source of oxygenated terminals which could easily tailored the surface roughness of  $\text{Co}_3\text{O}_4$  nanostructures. In the typical sodium citrate treatment, 5 g of  $\text{Co}_3\text{O}_4$  nanostructures were placed in 100 beaker capacity with 20 mL of 0.1M sodium citrate. The reducing agent treatment was carried out for two different times such as 1 and 1.5 h. After this, modified  $\text{Co}_3\text{O}_4$  nanostructures were collected on the filter paper, washed with the deionized water and dried for overnight. The treated  $\text{Co}_3\text{O}_4$  nanostructures for 1 and 1.5 hours were labeled as sample 1 and sample 2 respectively. The each step involved during the synthesis of surface modified  $\text{Co}_3\text{O}_4$  nanostructures is shown in Figure 1.

### **2.3. Structural and electrochemical measurements for ascorbic detection on citrate derived $\text{Co}_3\text{O}_4$ nanostructures**

The crystal quality aspects of  $\text{Co}_3\text{O}_4$  nanostructures were studied by powder X-ray diffraction (PXRD) with measurements conditions of  $\text{CuK}\alpha$  radiation ( $\lambda = 1.5418 \text{ \AA}$ ) 45 kV and 45 mA. A low resolution scanning electron microscopy was used under the experimental conditions of 20 kV to evaluate the surface morphology of as prepared  $\text{Co}_3\text{O}_4$  nanostructures. The  $\text{Co}_3\text{O}_4$  nanostructures catalyst ink was prepared by dissolving 0.10 mg of  $\text{Co}_3\text{O}_4$  nanostructures into 2.5 mL of deionized water and 0.5 mL of 5% Nafion. Then a homogenous catalyst ink was achieved in ultrasonic bath for 10 min. For the cleaning of glassy carbon electrode (GCE), it was polished with alumina paste (0.5 $\mu\text{m}$ ) and rubbed by silicon paper. Afterwards, GCE was washed several times with the deionized water. Then, drop cast method was used to deposit 10 $\mu\text{L}$  of  $\text{Co}_3\text{O}_4$  nanostructures onto GCE and it was labeled as modified (MGCE) and was used as a working electrode. The electrochemical experiments were done with three electrode cell configuration involving the silver-silver chloride ( $\text{Ag}/\text{AgCl}$ , 3.0M KCl) as reference electrode and platinum wire as a counter electrode. Keeping in consideration the physiological pH environment for the real sample analysis of ascorbic acid in human body, hence we used the phosphate buffer

solution of pH 7.4. Also from the previous works, it has been shown that the electrochemical detection of ascorbic acid is more favorable around pH of 7.3 – 7.4. Different ascorbic acid concentrations were made in phosphate buffer solution of pH 7.4. The phosphate buffer solution of pH 7.4 was used as a supporting electrolyte. Different electrochemical modes were used such as cyclic voltammetry (CV), linear sweep voltammetry (LSV) and chronoamperometry. The real sample analysis was also done on the MGCE for the quantification of ascorbic acid from human urine sample. The real sample was collected by healthy voluntary person from our laboratory and the preparation was done by adding 1 mL of human urine sample in 19 mL of phosphate buffer solution of pH 7.4. Then, it was analyzed by presented non-enzymatic ascorbic acid sensor.

### **3. Results and discussions**

#### **3.1. Morphology, and crystalline characterization of oxygenated terminals treated Co<sub>3</sub>O<sub>4</sub> nanostructures**

The reaction mechanism of ascorbic acid onto the Co<sub>3</sub>O<sub>4</sub> nanostructures takes place by the transfer of two electrons and protons as shown in Figure 2 and it has been generally represented in the previous studies [3, 4]. The Nernst equation has been used to describe the equal number of protons and electrons transfer during the oxidation of ascorbic acid as given under:

$$\text{Nernst equation, } E_p \text{ (V)} = -0,059 \text{ (m/n) pH} + E^0 \quad \text{Eq(1)}$$

Here  $E_p$  is peak potential, m and n are the number of protons and electrons. The ascorbic acid molecules were adsorbed on the modified GCE when it was inserted in the ascorbic acid solution, then the applied potential favored the oxidation of ascorbic acid into dehydroascorbic acid. At the same time, electrons and protons were produced, consequently the free electrons contributed towards the enhanced conductance of MGCE and also electron transfer kinetics as shown in Figure 2. During the electrochemical reaction of ascorbic acid on MGCE of Co<sub>3</sub>O<sub>4</sub> nanostructures, the formation of cobalt (II) hydroxide and further its oxidation into CoOOH could be expected, hence such phenomenon has been considered to monitor the detection of ascorbic acid using non-enzymatic approach. The morphology of modified Co<sub>3</sub>O<sub>4</sub> nanostructures

was evaluated by SEM as shown in Figure 3. The SEM image of pristine  $\text{Co}_3\text{O}_4$  nanostructures without sodium citrate (sample-1) exhibited porous flower like structure with dimension of few microns as shown in Figure 3a. However, the citrate ion treated  $\text{Co}_3\text{O}_4$  nanostructures with different time intervals like 1 and 1.5 h were also studied by SEM and their corresponding SEM images are shown in Figure 3 (b, c). The citrate ions have made the surface of  $\text{Co}_3\text{O}_4$  nanostructures relatively rough due to its reducing aspects of sodium citrate and these changes are highly visible for the sample 2 and 3 through SEM images as shown in Figure 3(b,c). The surface modification of  $\text{Co}_3\text{O}_4$  nanostructures after hydrothermal synthesis has not been investigated and the present approach offers a facile approach for the surface modification of nanostructured materials. The significant heterogeneity on the surface of  $\text{Co}_3\text{O}_4$  could be seen from Figure (3b,c), and it could be useful for the electrochemical applications. These surface alterations further proved to be an effective tool for the development of non-enzymatic ascorbic acid sensor in the presented work. To investigate the purity and crystal quality of as prepared  $\text{Co}_3\text{O}_4$  materials, powder XRD technique was performed as shown in Figure 3(d). The experiment was performed at  $2\theta$  angle range with scanning from  $30$  to  $80^\circ$ . The XRD study has shown that there is an effect on the intensity of diffraction patterns when sodium citrate was used and the some of the reflections of  $\text{Co}_3\text{O}_4$  were become more intense, suggesting the improved crystal quality compare to the pristine  $\text{Co}_3\text{O}_4$ . The diffraction patterns of  $\text{Co}_3\text{O}_4$  were fully agreed with the standard JCPDS card (96-900-5889). The  $\text{Co}_3\text{O}_4$  samples were identified with cubic crystal phase and there was no any other impurity in the samples, suggesting high quality of as prepared  $\text{Co}_3\text{O}_4$  material.

### **3.2. Electrochemical measurements for the determination of ascorbic acid using surface modified $\text{Co}_3\text{O}_4$ nanostructures**

The CV curves at a scan rate of  $50 \text{ mV/s}$  were measured for the  $\text{Co}_3\text{O}_4$  nanostructures in the absence and presence of ascorbic acid in phosphate buffer solution of pH 7.4. The CV curves of pristine  $\text{Co}_3\text{O}_4$  nanostructures (sample 1), surface modified  $\text{Co}_3\text{O}_4$  nanostructures (sample 2, sample 3) deposited onto GCE were recorded in  $0.1 \text{ mM}$  ascorbic acid as shown in Figure 4a. The electrocatalytic properties of three samples of  $\text{Co}_3\text{O}_4$  nanostructures were studied by CV curves and sample 3 was found with enhanced oxidation peak current and well-shaped peak as shown in Figure 4a. Further to verify, whether peak is coming mainly from ascorbic acid or

electrolyte, hence we only tested sample 3 in the electrolyte without ascorbic acid and with the use of ascorbic acid as shown in Figure 4b. The sample 3 has shown non-Faradic process in the supporting electrolyte, however it has described well resolved oxidation peak in the ascorbic acid, suggesting its superior redox electrochemical activity as shown in Figure 4b. The surface area and excellent compatibility of newly prepared  $\text{Co}_3\text{O}_4$  nanostructures with the surface of GCE have played a vital role towards the superior performance during non-enzymatic sensing of ascorbic acid in the presented study. Moreover, an enhanced surface roughness and also improved catalytic properties of  $\text{Co}_3\text{O}_4$  nanostructures played an outstanding role for the sensitive detection of ascorbic acid. Furthermore, we have studied the Faradic kinetics of  $\text{Co}_3\text{O}_4$  nanostructures (sample 3) through CV curves at various scan rates ranging from 10-80 mV/s in 0.1 mM ascorbic acid as shown in Figure 5a. It was observed that the oxidation peak current was increasing with each rise of scan rate, suggesting the well behaved diffusion electrochemical process on the modified electrode. . The plot of oxidation peak current enhancement with each scan rate was plotted against the square root of scan root as shown in Figure 5b, indicating the well analytical features of modified GCE [33, 34]. The working range of newly developed non-enzymatic ascorbic acid sensor based on  $\text{Co}_3\text{O}_4$  nanostructures was also evaluated in phosphate buffer solution of pH 7.4. Various CV curves measured at scan rate of 50 mV/s in the different concentrations of ascorbic acid as shown in Figure 6a. It was obvious that the oxidation peaks were increasing linearly with each rise in increment of ascorbic acid concentration, verifying the sensitive signal of sample 3 against the ascorbic acid molecules. The linear plot of oxidation peak current of each CV curve was fitted against the ascorbic acid concentrations and well defined analytical fitting features were observed through the regression coefficient of 0.99. This confirms an excellent analytical behavior of presented electroanalytical method based on  $\text{Co}_3\text{O}_4$  nanostructures as shown in Figure 6b. A wide linear range of 0.1mM -6.5mM ascorbic acid concentration using CV measurement. The low limit of detection was estimated by published work [35], and it was found about 0.001 mM. The linear range and low limit of detection of presented ascorbic acid sensor were superior to many of the published ascorbic acid sensors using various nanostructured materials like Pt-Ti alloy [36, 37, 38]. In the CV curves, Faradic current is directly used to quantify the kinetics of electrochemical process occurring on the surface of working electrode. Moreover, the peak current is depending on the speed at which electrode material receives number of molecules from the bulk solution of analyte which are connected to mass transport. It has been shown that at low concentration of analyte, diffusion

takes place without disturbance, hence peak shift could not take places. However, diffusion is highly disrupted at higher concentrations, thus it offers big barrier for the favorable mass transport and it has compensated by disruptive diffusion. Therefore, the reoccurrence of mass transport without the disturbance and electrochemical reaction needs more potential, thus it causes shift in the peak potential. Furthermore, the electrochemical reaction needs a particular time span to assure the diffusion of reactive species and the charge transfer on the surface of working electrode. Therefore, the shift in the potential could be attributed to the delay of electrochemical process because of the shortness of given time compare to the time given to electrochemical reaction at lower concentration or scan rate. The intersection of CV curves for 6 mM and 6.5 mM concentrations could be indexed to the shift in the peak potential towards low overpotential for 6.5 mM concentration, hence it seems that there is intersection. The calibration of various ascorbic acid concentrations was also made with the use of linear sweep voltammetry (LSV) as shown in Figure 7a. It is clear that the CV results for calibration were further found in good agreement with LSV results and offered another aspect of sensitivity of  $\text{Co}_3\text{O}_4$  nanostructures. Interestingly, the LSV results become very much sensitive owing to their higher working range from 0.1- 6.5 mM as shown by linear fitting of oxidation peak current form LSV curves versus different ascorbic acid concentrations as shown in Figure 7b. Furthermore, the calibration plot was obtained by using chronoamperometry which is more sensitive electrochemical method and the observed results are shown in Figure 8a. Each chronoamperometric response suggests the successive increase in the current related to rise in the concentration of ascorbic acid, indicating the excellent electrocatalytic properties of  $\text{Co}_3\text{O}_4$  nanostructures tuned by the treatment of sodium citrate. We have also plotted linear fitting through the increase in the current during chronoamperometric signal against various ascorbic acid concentrations as shown in Figure 8b. The linear fitting revealed highly sensitive nature of  $\text{Co}_3\text{O}_4$  nanostructures by demonstrating linear range of 1-5 mM of ascorbic acid. The chronoamperometry results suggest that the each i-t curve response time is highly durable and could be applied for certain period of time for the detection of ascorbic acid.

The selectivity of as prepared  $\text{Co}_3\text{O}_4$  nanostructures towards ascorbic acid detection was studied under the environment of competing interfering agents such as uric acid, potassium ions, sodium ions, ethanol, lactic acid, urea and glucose as shown in Figure 9a. For the selectivity measurement, 0.1mM ascorbic acid solution and other interring agents was used and standard

addition method was used to record the change in the oxidation peak current during the record of CV curves as shown in Figure 8a. From this analysis, it is obvious that less than 3% change in the peak current was noticed with the addition of these interfering species, consequently the prepared  $\text{Co}_3\text{O}_4$  nanostructures have shown selective response towards the detection of ascorbic acid. Hence, the presented non-enzymatic ascorbic acid sensor has high capability to quantify ascorbic acid from complex matrixes of real samples. The stability of  $\text{Co}_3\text{O}_4$  nanostructures was also evaluated in 0.1mM ascorbic acid by measuring different CV curves at the scan rate of 50 mV/s as shown in Figure 9b. The good stability could be attributed to the fact that sodium citrate has added the significant surface roughness of  $\text{Co}_3\text{O}_4$  nanostructures which firmly bound with the surface of GCE, consequently we have observed an excellent stability. For better analytical representation, the same stability results of CV analysis were further described by bar graph using error bar as shown in Figure 9c, suggesting acceptable relative standard deviation (RSD) value of less than 1%. From 13 CV cycles of same MGCE has indicated the significant repeatable capability of electrode during stability measurement.

To study the practical aspects of as developed non-enzymatic ascorbic acid sensor for the determination of ascorbic acid for human urine sample using recovery (%) method as given in Table 1. The recoveries of proposed  $\text{Co}_3\text{O}_4/\text{GCE}$  were found close to 100%. The stability and reproducibility could be seen from the relative standard deviation (RSD) data as given in Table 1. All concrete values of RSD are less than 1%, suggesting the potential practical application of as developed MGCE for the determination of ascorbic acid. It further confirms the real sample analysis of as presented non-enzymatic ascorbic acid sensor. The RSD (%) was calculated as (standard deviation/mean of measured data by 3 repeated measurements)  $\times 100\%$ .

**Table 1:** Recovery (%) of ascorbic acid from urine sample using proposed  $\text{Co}_3\text{O}_4/\text{GCE}$  non-enzymatic sensor

Sample (Urine)	Added (mM)	Found (mM)	Recovery (%)	RSD(%)
1	0.523	0.521 $\pm$ 0.0085	100.38	0.471
2	1.084	1.091 $\pm$ 0.0068	100.64	0.563
3	1.532	1.541 $\pm$ 0.0075	100.58	0.524

For the simplicity, we have provided the comparison analysis of our presented results with reported works as shown in Table 2. The quantitative information about the performance of presented non-enzymatic ascorbic acid sensor was collected by the comparative analysis as given in Table 2 [23, 13-37, 4, 38-44]. From the previous studies about the determination of ascorbic acid, it can be seen that the composite systems have been used which are complicated and highly expensive to characterize compare to the presented non-enzymatic ascorbic acid sensor. The  $\text{Co}_3\text{O}_4$  nanostructures (sample 3) has demonstrated a wide linear range which was verified by different electrochemical modes, confirming their high potential towards the practical applications. This comparative analysis revealed better performance of  $\text{Co}_3\text{O}_4$  nanostructures (sample 3) and it can be connected to strong surface modification of  $\text{Co}_3\text{O}_4$  nanostructures by the citrate anions. The improved performance of  $\text{Co}_3\text{O}_4$  nanostructures could be attributed from the surface defects, and surface roughness as verified by SEM analysis. Moreover, the citrate ion treated  $\text{Co}_3\text{O}_4$  nanostructures significant crystal quality, thereby it played a vital role in driving the ascorbic oxidation reaction.

**Table 2:** The comparative study of presented ascorbic acid detection results with already published results of ascorbic acid using different materials

<b>Electrode Material</b>	<b>Linear range (<math>\mu\text{M}</math>)</b>	<b>Detection limit (<math>\mu\text{M}</math>)</b>	<b>Reference</b>
Pd/CNF-CPE <sup>a</sup>	50- 4000	15	[25]
Chitosan-graphene	50- 1200	50	[36]
OMC/Nafion <sup>b</sup>	40- 800	20	[37]
Carbon nanotube Voltametric	80- 1360	20	[38]
Nitrogen doped graphene (NG)/GCE	5- 1300	2.2	[39]
Au/Ru nanoshells/GCE	5- 2000	2.2	[2]
RGO/GCE <sup>d</sup>	30–350	14.8	[40]
ferrocene methanol/CNTY	3-3000	1.32	[41]
MWCNT/CCE <sup>e</sup>	15–800	7.71	[42]

RGO-ZnO/GCE <sup>f</sup>	50-2350	3.71	[43]
RGO-CD-MWCNT- POM <sup>g</sup>	5-2000	0.84	[44]
Co <sub>3</sub> O <sub>4</sub> /GCE	500- 6500	1	This work

<sup>a</sup> Palladium particles- deposited on carbon nanofiber and used for the modification of carbon paste electrode.

<sup>b</sup> Ordered mesoporous carbon/Nafion composite film.

<sup>c</sup> gold nanoparticles functionalized beta cyclodextrin graphene oxide onto glass carbon electrode

<sup>d</sup>Reduced graphene oxide/glassy carbon electrode

<sup>e</sup>MWCNTs: carboxylated multi-walled carbon nanotubes, PANI: polyaniline

<sup>f</sup>Reduced graphene oxide- ZnO/glassy carbon electrode

<sup>g</sup>Reduced graphene oxide/ $\beta$ -cyclodextrin/multiwall carbon nanotubes/ polyoxometalate

#### 4. Conclusions

In this study, we have employed a low cost surface modifying agent sodium citrate with high density of oxygenated terminals and it has significantly modified the surface properties of Co<sub>3</sub>O<sub>4</sub> nanostructures. Furthermore, the citrate ions have enhanced the electrochemical properties of Co<sub>3</sub>O<sub>4</sub> nanostructures towards the development of non-enzymatic ascorbic acid sensor. The structural analysis was carried out using low resolution SEM and powder XRD techniques. The treated Co<sub>3</sub>O<sub>4</sub> nanostructures exhibited rough surface compare to the pristine Co<sub>3</sub>O<sub>4</sub> nanostructures, confirming the significant surface modifications. The Co<sub>3</sub>O<sub>4</sub> nanostructures were observed with enhanced crystal properties. The Co<sub>3</sub>O<sub>4</sub> nanostructures have proved to be an excellent protocol for the sensitive and selective determination of ascorbic acid owing to their strong surface roughness, high surface area and excellent compatibility with the surface of GCE. The linear range of Co<sub>3</sub>O<sub>4</sub> nanostructures for the ascorbic acid detection was found from 0.5 mM to 6.5 mM using CV and LSV electrochemical modes. Beside this, the Co<sub>3</sub>O<sub>4</sub> nanostructures were characterized with low limit of detection of 0.001 mM, high stability and selectivity. The surface modification of Co<sub>3</sub>O<sub>4</sub> nanostructures using oxygenated groups is facile, low cost, and ecofriendly approach for the wide range of applications such as biomedical, energy conversion and storage systems.

## **Acknowledgement**

Authors are highly acknowledge higher education commission Pakistan for partial support under the project (NRPU/8350). We also extend our sincere appreciation to the Researchers Supporting Project number (RSP-2023/79) at King Saud University, Riyadh, Saudi Arabia.

## **6. Conflict of interest**

Authors declare no conflict of interest in this research work

## **Figure Captions**

**Figure 1:** Schematic diagram for the preparation of S1, S2 and S3 samples of  $\text{Co}_3\text{O}_4$  nanostructures and their electrochemical characterization

**Figure 2:** Illustration for the oxidation of ascorbic acid using proposed  $\text{Co}_3\text{O}_4$  nanostructures

**Figure 3:** SEM images of various  $\text{Co}_3\text{O}_4$  nanostructures (a) sample-1, (b) sample-2, (c) sample-3, (d) the corresponding of XRD patterns

**Figure 4: (a).** Cyclic Voltammogram of MGCE at scan rate of 50 mV/s with untreated S1, treated (S2 and S3) in 0.1 mM ascorbic acid, **(b).** Cyclic Voltammogram of MGCE with sample-3 at scan rate of 50 mV/s in 0.1 mM ascorbic acid and in electrolyte

**Figure 5: (a).** Cyclic voltammogram of sample-3 (S3) with various scan rates in 0.1mM ascorbic acid, **(b).** Plot of oxidation of peak current versus square root of scan rate

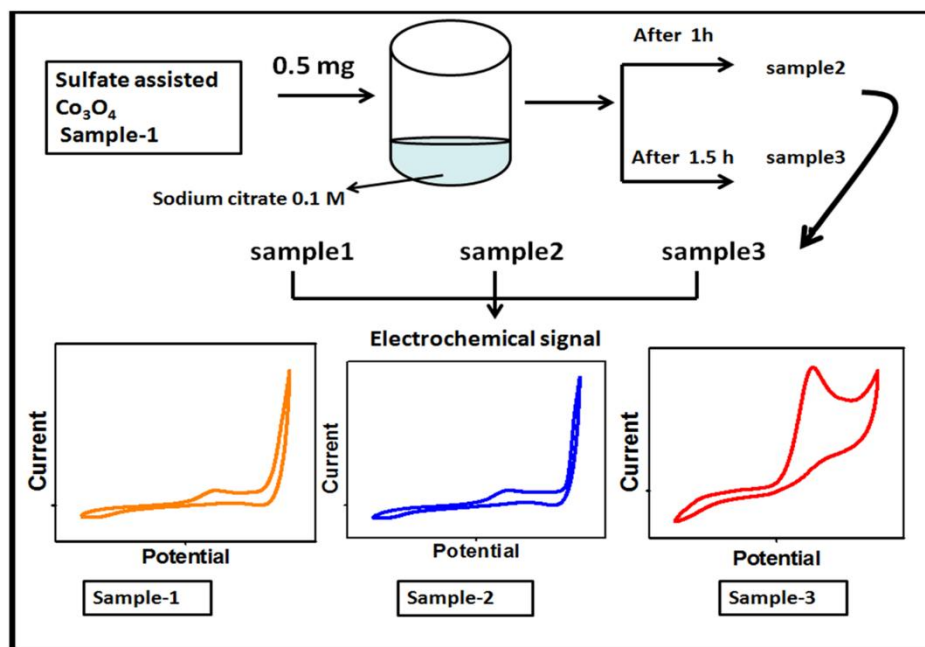
**Figure 6: (a).** Cyclic Voltammograms at different concentrations of ascorbic acid at a scan rate of 50 mV/s **(b).** Linear plot of oxidation peak current versus concentrations

**Figure 7: (a).** LSV at different concentrations of ascorbic acid at 10 mV/s **(b).** Linear fit of current at different concentrations of ascorbic acid

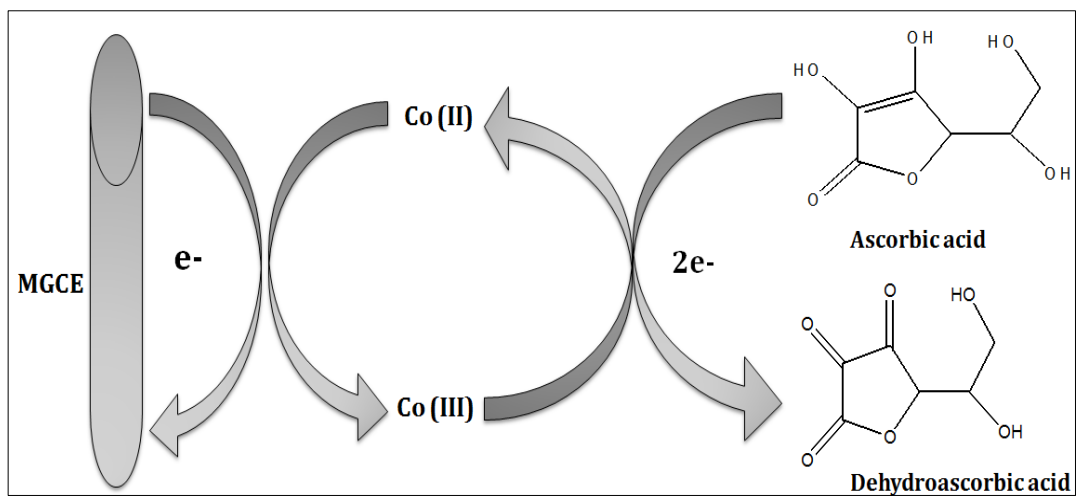
**Figure 8: (a).** chronoamperometric signal at different concentrations of ascorbic acid against 0.3 V (Ag/AgCl) **(b).** Linear plot of current versus concentration

**Figure 9: (a).** Cyclic Voltammogram of sample-3 in the presence and absence of different interfering substances at scan rate of 50 mV/s, **(b).** Cyclic Voltammogram sample-3 for measuring the stability in 0.1mM ascorbic acid at scan rate of 50 mV/s

**Figure 1:**



**Figure 2:**



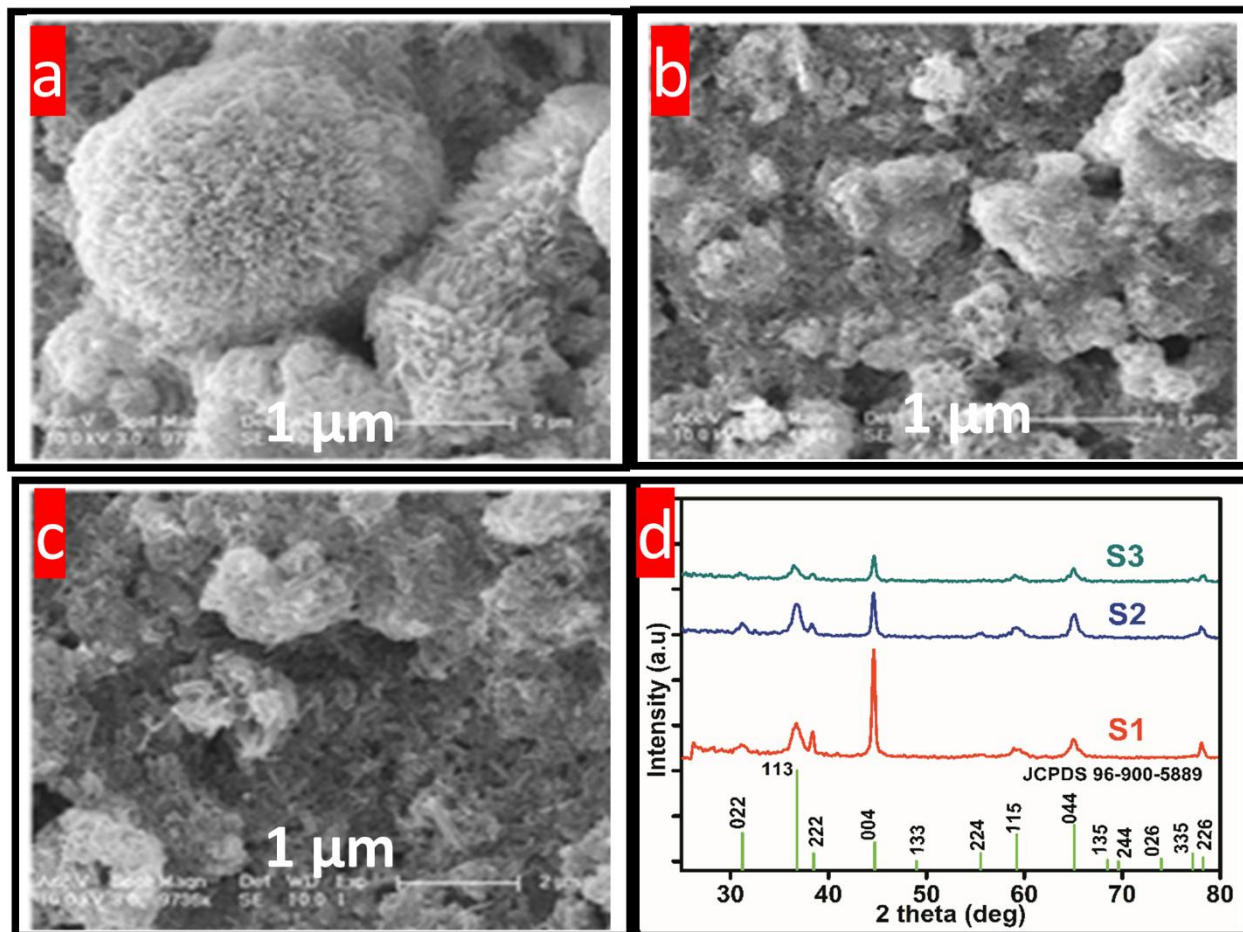


Figure 3:

Figure 4:

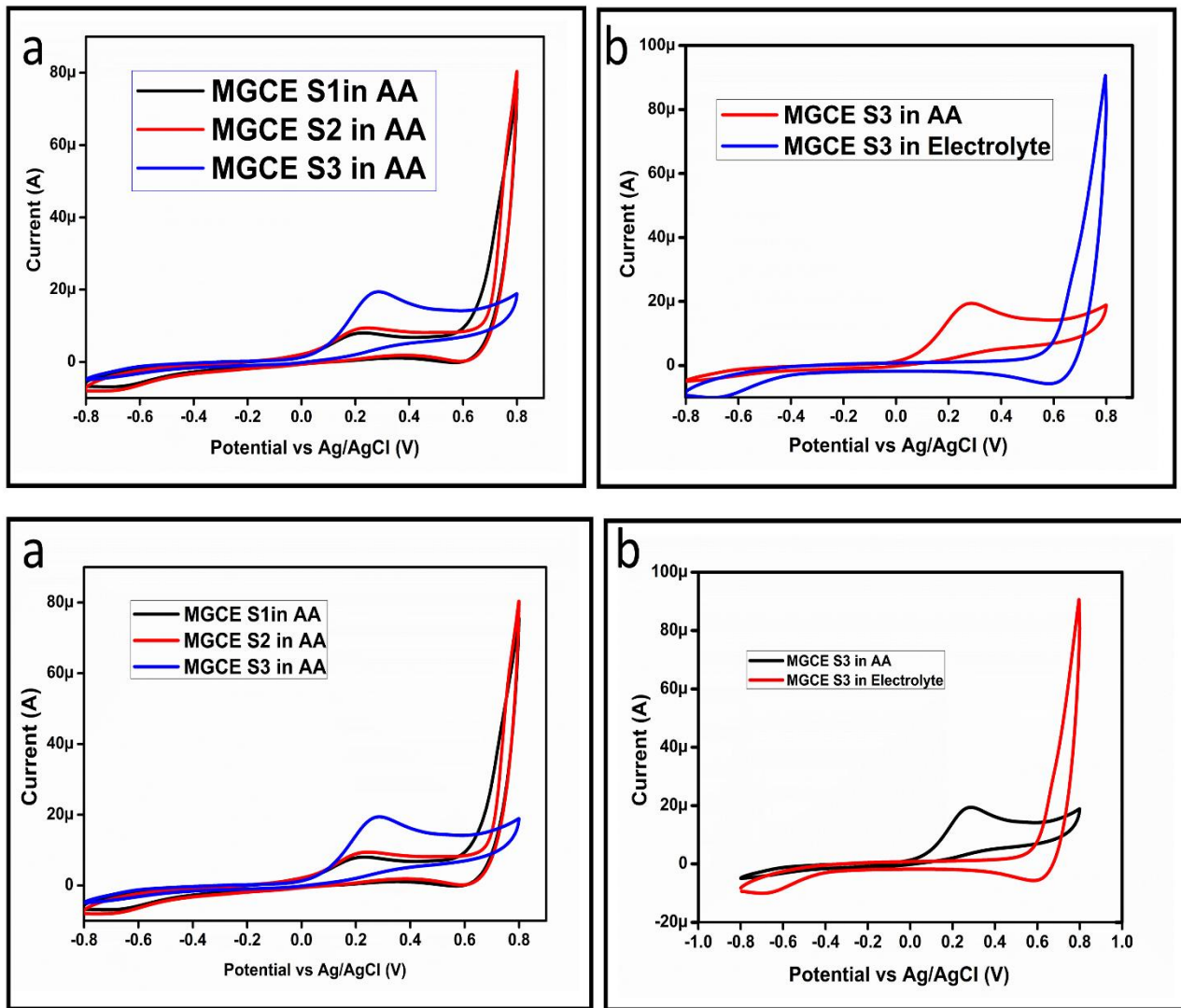


Figure 5:

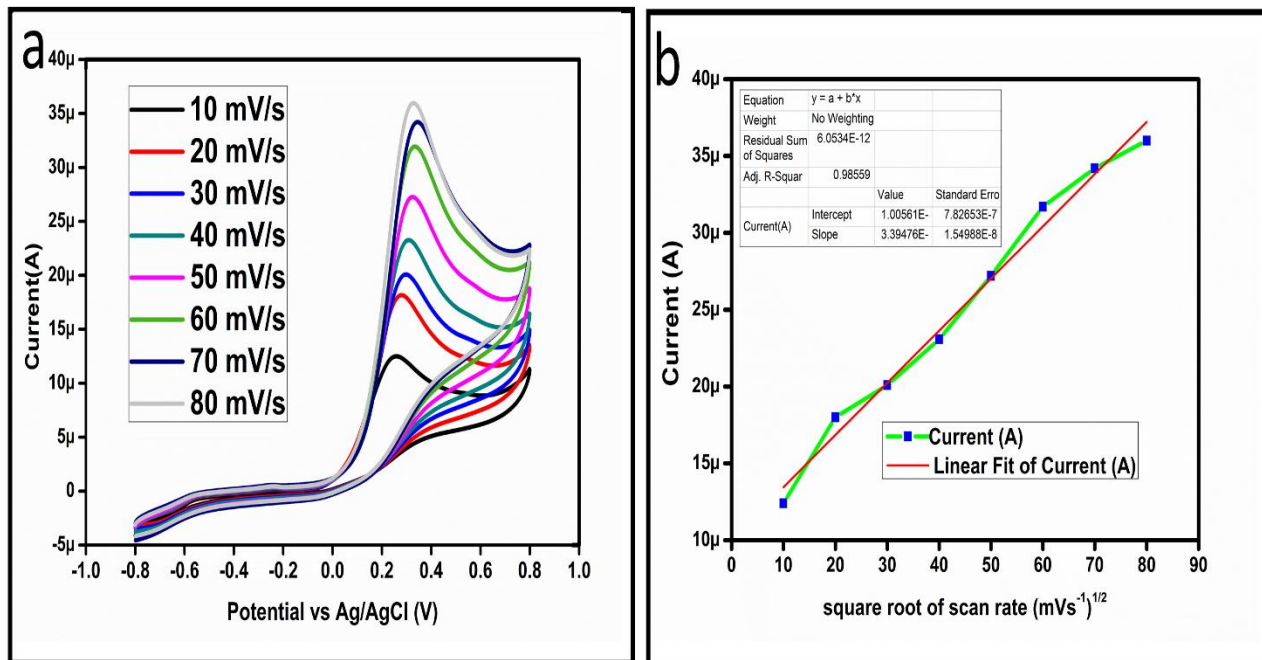


Figure 6:

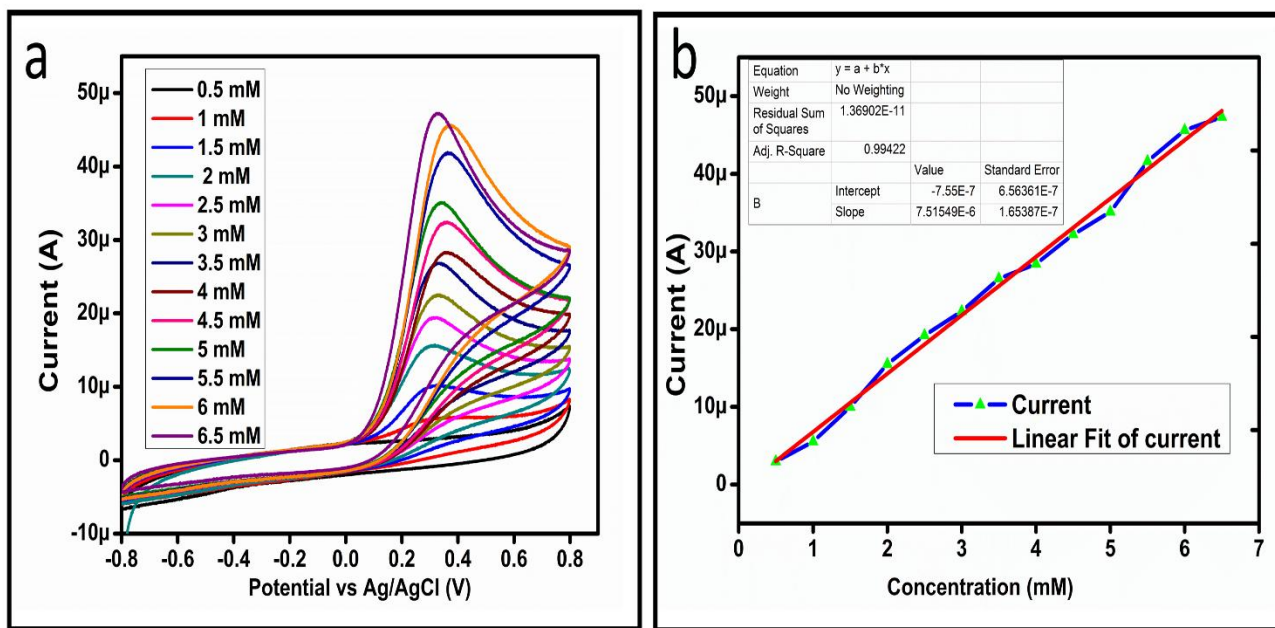


Figure 7:

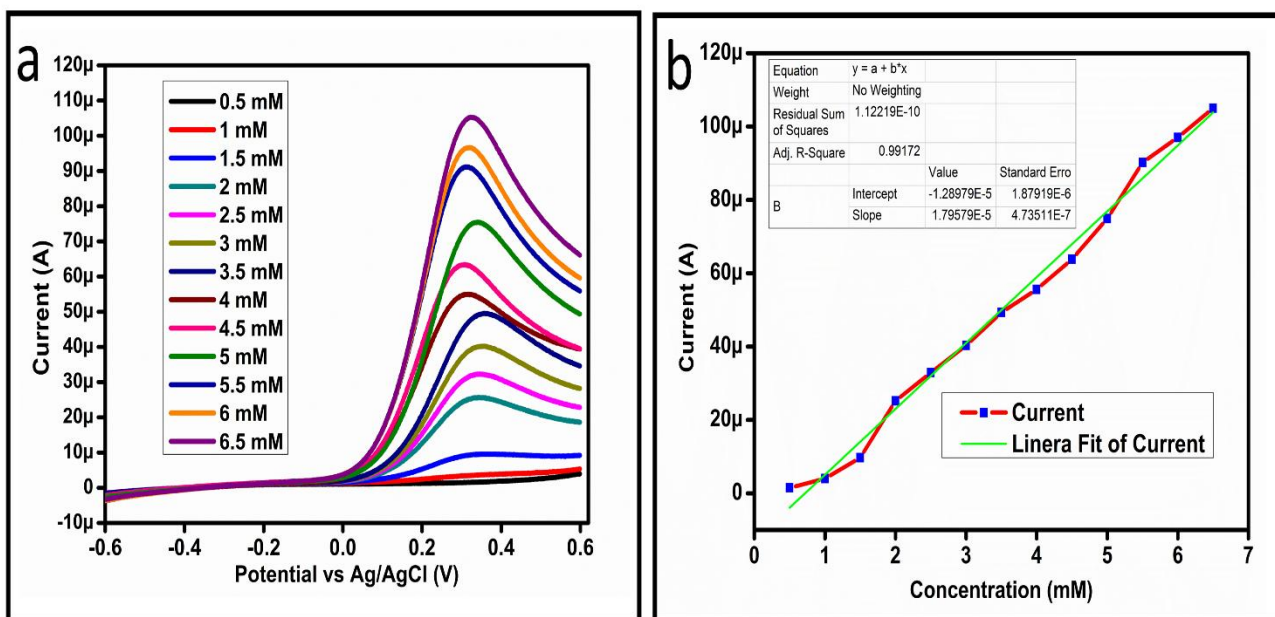


Figure: 8

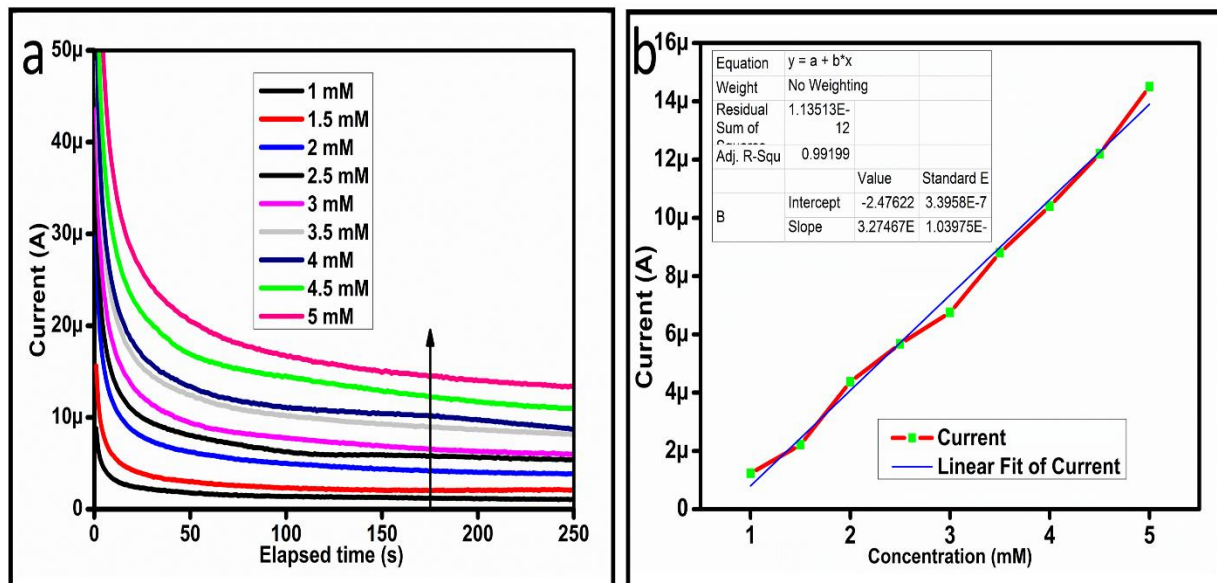
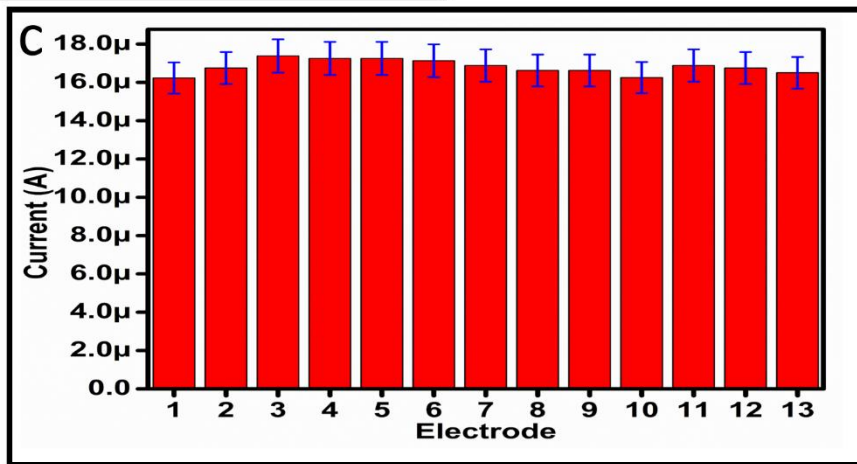
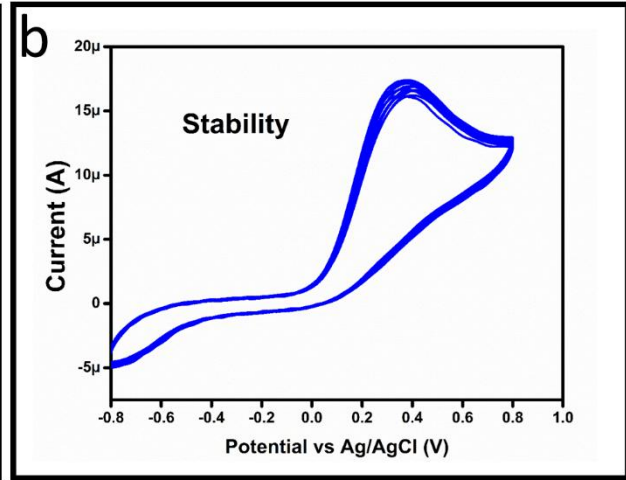
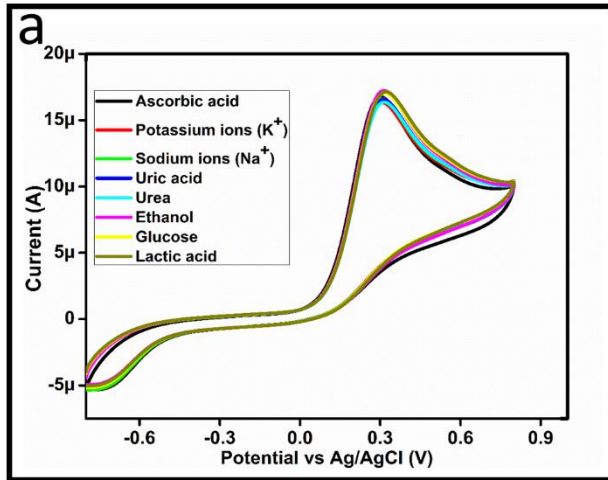


Figure 9:



## 5. References

1. Yogeswaran, U.; Thiagarajan, S.; Chen, S.-M., Nanocomposite of functionalized multiwall carbon nanotubes with nafion, nano platinum, and nano gold biosensing film for simultaneous determination of ascorbic acid, epinephrine, and uric acid. *Analytical biochemistry* **2007**, 365, (1), 122-131.
2. Jo, A.; Kang, M.; Cha, A.; Jang, H. S.; Shim, J. H.; Lee, N.-S.; Kim, M. H.; Lee, Y.; Lee, C., Nonenzymatic amperometric sensor for ascorbic acid based on hollow gold/ruthenium nanoshells. *Analytica chimica acta* **2014**, 819, 94-101.
3. Frenich, A. G.; Torres, M. H.; Vega, A. B.; Vidal, J. M.; Bolanos, P. P., Determination of ascorbic acid and carotenoids in food commodities by liquid chromatography with mass spectrometry detection. *Journal of agricultural and food chemistry* **2005**, 53, (19), 7371-7376.
4. Silva, F. O., Total ascorbic acid determination in fresh squeezed orange juice by gas chromatography. *Food Control* **2005**, 16, (1), 55-58.
5. Gai, S.; Yang, P.; Li, C.; Wang, W.; Dai, Y.; Niu, N.; Lin, J., Synthesis of Magnetic, Up-Conversion Luminescent, and Mesoporous Core-Shell-Structured Nanocomposites as Drug Carriers. *Advanced Functional Materials* **2010**, 20, (7), 1166-1172.
6. Wang, H.; Zhou, L.; Han, M.; Tao, Z.; Cheng, F.; Chen, J., CuCo nanoparticles supported on hierarchically porous carbon as catalysts for hydrolysis of ammonia borane. *Journal of Alloys and Compounds* **2015**, 651, 382-388.
7. Tian, X.; Cheng, C.; Yuan, H.; Du, J.; Xiao, D.; Xie, S.; Choi, M. M., Simultaneous determination of L-ascorbic acid, dopamine and uric acid with gold nanoparticles- $\beta$ -cyclodextrin-graphene-modified electrode by square wave voltammetry. *Talanta* **2012**, 93, 79-85.
8. Chauhan, N.; Narang, J.; Pundir, C., Fabrication of multiwalled carbon nanotubes/polyaniline modified Au electrode for ascorbic acid determination. *Analyst* **2011**, 136, (9), 1938-1945.
9. Keeley, G. P.; O'Neill, A.; McEvoy, N.; Peltekis, N.; Coleman, J. N.; Duesberg, G. S., Electrochemical ascorbic acid sensor based on DMF-exfoliated graphene. *Journal of Materials Chemistry* **2010**, 20, (36), 7864-7869.
10. Singh, A.; Sharma, A.; Ahmed, A.; Arya, S., Highly selective and efficient electrochemical sensing of ascorbic acid via CuO/rGO nanocomposites deposited on conductive fabric. *Applied Physics A* **2022**, 128, (4), 1-12.
11. Singh, A.; Ahmed, A.; Sharma, A.; Arya, S., Graphene and its derivatives: Synthesis and application in the electrochemical detection of analytes in sweat. *Biosensors* **2022**, 12, (10), 910.
12. Kumar, S. A.; Lo, P.-H.; Chen, S.-M., Electrochemical selective determination of ascorbic acid at redox active polymer modified electrode derived from direct blue 71. *Biosensors and Bioelectronics* **2008**, 24, (4), 518-523.
13. Luo, X.-L.; Xu, J.-J.; Zhao, W.; Chen, H.-Y., Ascorbic acid sensor based on ion-sensitive field-effect transistor modified with MnO<sub>2</sub> nanoparticles. *Analytica chimica acta* **2004**, 512, (1), 57-61.
14. Singh, A.; Sharma, A.; Ahmed, A.; Sundramoorthy, A. K.; Furukawa, H.; Arya, S.; Khosla, A., Recent advances in electrochemical biosensors: Applications, challenges, and future scope. *Biosensors* **2021**, 11, (9), 336.
15. Greenway, G. M.; Ongomo, P., Determination of L-ascorbic acid in fruit and vegetable juices by flow injection with immobilised ascorbate oxidase. *Analyst* **1990**, 115, (10), 1297-1299.
16. Fang, C.; Tang, X.; Zhou, X., Preparation of poly (malachite green) modified electrode and the determination of dopamine and ascorbic acid. *Analytical sciences* **1999**, 15, (1), 41-46.
17. Gao, Z.; Yap, D.; Zhang, Y., Voltammetric determination of dopamine in a mixture of dopamine and ascorbic acid at a deactivated polythiophene film modified electrode. *Analytical sciences* **1998**, 14, (6), 1059-1063.

18. Gupta, J.; Arya, S.; Verma, S.; Singh, A.; Sharma, A.; Singh, B.; Sharma, R., Performance of template-assisted electrodeposited Copper/Cobalt bilayered nanowires as an efficient glucose and Uric acid sensor. *Materials Chemistry and Physics* **2019**, 238, 121969.
19. Kiran, S.; Misra, R., Mechanism of intracellular detection of glucose through nonenzymatic and boronic acid functionalized carbon dots. *Journal of Biomedical Materials Research Part A* **2015**, 103, (9), 2888-2897.
20. Bao, L.; Li, T.; Chen, S.; Peng, C.; Li, L.; Xu, Q.; Chen, Y.; Ou, E.; Xu, W., 3D Graphene Frameworks/Co3O4 Composites Electrode for High-Performance Supercapacitor and Enzymeless Glucose Detection. *Small* **2017**, 13, (5), 1602077.
21. Srinivasan, V.; Weidner, J. W., Capacitance studies of cobalt oxide films formed via electrochemical precipitation. *Journal of power sources* **2002**, 108, (1-2), 15-20.
22. Tyczkowski, J.; Kapica, R.; Łojewska, J., Thin cobalt oxide films for catalysis deposited by plasma-enhanced metal-organic chemical vapor deposition. *Thin Solid Films* **2007**, 515, (16), 6590-6595.
23. Okabe, H.; Akimitsu, J.; Kubodera, T.; Matoba, M.; Kyomen, T.; Itoh, M., Low-temperature magnetoresistance of layered cobalt oxides  $\text{Na}_x\text{CoO}_2$ . *Physica B: Condensed Matter* **2006**, 378, 863-864.
24. Kadam, L.; Pawar, S.; Patil, P., Studies on ionic intercalation properties of cobalt oxide thin films prepared by spray pyrolysis technique. *Materials chemistry and physics* **2001**, 68, (1-3), 280-282.
25. Huang, J.; Liu, Y.; Hou, H.; You, T., Simultaneous electrochemical determination of dopamine, uric acid and ascorbic acid using palladium nanoparticle-loaded carbon nanofibers modified electrode. *Biosensors and Bioelectronics* **2008**, 24, (4), 632-637.
26. Kang, L.; He, D.; Bie, L.; Jiang, P., Nanoporous cobalt oxide nanowires for non-enzymatic electrochemical glucose detection. *Sensors and Actuators B: Chemical* **2015**, 220, 888-894.
27. Wang, X.; Dong, X.; Wen, Y.; Li, C.; Xiong, Q.; Chen, P., A graphene-cobalt oxide based needle electrode for non-enzymatic glucose detection in micro-droplets. *Chemical Communications* **2012**, 48, (52), 6490-6492.
28. Kim, S.; Yang, W. S.; Kim, H.-J.; Lee, H.-N.; Park, T. J.; Seo, S.-J.; Park, Y. M., Highly sensitive non-enzymatic lactate biosensor driven by porous nanostructured nickel oxide. *Ceramics International* **2019**, 45, (17), 23370-23376.
29. Zahed, M. A.; Barman, S. C.; Toyabur, R.; Sharifuzzaman, M.; Xuan, X.; Nah, J.; Park, J. Y., Ex Situ Hybridized Hexagonal Cobalt Oxide Nanosheets and RGO@ MWCNT Based Nanocomposite for Ultra-Selective Electrochemical Detection of Ascorbic Acid, Dopamine, and Uric Acid. *Journal of The Electrochemical Society* **2019**, 166, (6), B304-B311.
30. Nguyen, N. S.; Das, G.; Yoon, H. H., Nickel/cobalt oxide-decorated 3D graphene nanocomposite electrode for enhanced electrochemical detection of urea. *Biosensors and Bioelectronics* **2016**, 77, 372-377.
31. Aftab, A .K.; Saeed, A. L.; Aneela,T.; Mohd, U.; Asma, A.; Khoulwod, A.; Ayman, N.; Zafar, H. I.; Facile Electrochemical Determination of Methotrexate (MTX) Using Glassy Carbon Electrode-Modified with Electronically Disordered NiO Nanostructures, *Nanomaterials* 2021, 11, 1266; <https://doi.org/10.3390/nano11051266>
32. Aftab, A .K.; Saeed, A. L.; Aneela,T.; Mansoor, A.; Umair, A.; Muhammad, I.A.; Awais, A.J.; Ayman. N.; Zafar, H I.; Synthesis of Sheet Like Nanostructures of NiO Using Potassium Dichromate as Surface Modifying Agent for the Sensitive and Selective Determination of Amlodipine Besylate (ADB) Drug, *Electroanalysis*, 33, 202, 1121-1128
33. dos Santos, P. L.; Katic, V.; Toledo, K. C.; Bonacin, J. A., Photochemical one-pot synthesis of reduced graphene oxide/Prussian blue nanocomposite for simultaneous electrochemical detection of ascorbic acid, dopamine, and uric acid. *Sensors and Actuators B: Chemical* **2018**, 255, 2437-2447.

34. Lim, C. X.; Hoh, H. Y.; Ang, P. K.; Loh, K. P., Direct voltammetric detection of DNA and pH sensing on epitaxial graphene: an insight into the role of oxygenated defects. *Analytical chemistry* **2010**, *82*, (17), 7387-7393.
35. Sidra, A.; Aneela, T.; Amber, R. S.; Raffaello, M.; Zafar, H. I.; Almas, F.; Alberto, V.; Functional nickel oxide nanostructures for ethanol oxidation in alkaline media, *Electroanalysis*, *32*, 2020, 1052-1059
36. Han, D.; Han, T.; Shan, C.; Ivaska, A.; Niu, L., Simultaneous determination of ascorbic acid, dopamine and uric acid with chitosan-graphene modified electrode. *Electroanalysis* **2010**, *22*, (17-18), 2001-2008.
37. Zheng, D.; Ye, J.; Zhou, L.; Zhang, Y.; Yu, C., Simultaneous determination of dopamine, ascorbic acid and uric acid on ordered mesoporous carbon/Nafion composite film. *Journal of Electroanalytical Chemistry* **2009**, *625*, (1), 82-87.
38. Wang, Z.; Liu, J.; Liang, Q.; Wang, Y.; Luo, G., Carbon nanotube-modified electrodes for the simultaneous determination of dopamine and ascorbic acid. *Analyst* **2002**, *127*, (5), 653-658.
39. Sheng, Z.-H.; Zheng, X.-Q.; Xu, J.-Y.; Bao, W.-J.; Wang, F.-B.; Xia, X.-H., Electrochemical sensor based on nitrogen doped graphene: simultaneous determination of ascorbic acid, dopamine and uric acid. *Biosensors and Bioelectronics* **2012**, *34*, (1), 125-131.
40. Tukimin, N.; Abdullah, J.; Sulaiman, Y., Electrodeposition of poly (3, 4-ethylenedioxythiophene)/reduced graphene oxide/manganese dioxide for simultaneous detection of uric acid, dopamine and ascorbic acid. *Journal of Electroanalytical Chemistry* **2018**, *820*, 74-81.
41. Wang, Y.; Wu, J.; Yang, T.; Wang, Z.; Hasebe, Y.; Lv, T.; Zhang, Z., A Novel Flexible Electrochemical Ascorbic Acid Sensor Constructed by Ferrocene Methanol doped Multi-walled Carbon Nanotube Yarn. *Electroanalysis* **2021**, *33*, (12), 2445-2451.
42. Habibi, B.; Pournaghi-Azar, M. H., Simultaneous determination of ascorbic acid, dopamine and uric acid by use of a MWCNT modified carbon-ceramic electrode and differential pulse voltammetry. *Electrochimica Acta* **2010**, *55*, (19), 5492-5498.
43. Zhang, X.; Zhang, Y.-C.; Ma, L.-X., One-pot facile fabrication of graphene-zinc oxide composite and its enhanced sensitivity for simultaneous electrochemical detection of ascorbic acid, dopamine and uric acid. *Sensors and Actuators B: Chemical* **2016**, *227*, 488-496.
44. Ma, C.; Xu, P.; Chen, H.; Cui, J.; Guo, M.; Zhao, J., An electrochemical sensor based on reduced graphene oxide/ $\beta$ -cyclodextrin/multiwall carbon nanotubes/polyoxometalate tetracomponent hybrid: Simultaneous determination of ascorbic acid, dopamine and uric acid. *Microchemical Journal* **2022**, *180*, 107533.